Z scan using circularly symmetric beams

Bum Ku Rhee and Jin Seob Byun

Department of Physics, Sogang University, Seoul 121-742, Korea

E. W. Van Stryland

Center for Research in Electro-Optics and Lasers, University of Central Florida, Orlando, Florida 32816

Received December 20, 1995; revised manuscript received June 4, 1996

We report general characteristics of on-axis Z-scan transmittance for arbitrary circularly symmetric beams. Some experimental results are presented for a nearly top-hat-shaped beam and for a trimmed Airy beam whose electric field profile is the central portion of an Airy function inside its first zero. The sensitivity of Z-scan method with a trimmed Airy beam for measuring an induced index-of-refraction change is a factor of 1.5 greater than that of a Gaussian beam. Also, it is found that there are some advantages of experimental alignment and numerical convergence for a Z-scan measurement that uses a trimmed Airy beam over one that uses a top-hat beam. © 1996 Optical Society of America.

Since the Z-scan method[1,2] was developed, it has been widely applied to measure optically induced phase distortion in $\chi^{(3)}$ for various materials because of its simplicity and accuracy.[3–5] In 1993 Zhao and Palffy-Muhoray[6] extended its application to top-hat beams, whereas most Z-scan experiments and their analyses were performed for Gaussian beams.

We report some general characteristics of on-axis transmittance when a Z scan is carried out with circularly symmetric beams and present the corresponding experimental results for laser beams of spatially nearly top-hat and trimmed Airy profiles. Throughout this study, only on-axis Z-scan transmittance will be considered, which we have experimentally approximated by using a small aperture placed in the far field. First we derive the on-axis Z-scan transmittance formally for an arbitrary circularly symmetric beam and describe the corresponding Z-scan experiments with CS_2 in detail. Then we compare the experimental results with numerical predictions and discuss some advantages of Z-scan measurement using a trimmed Airy beam compared with one using a top-hat beam.

For the Z-scan experiment a well-collimated beam (input beam) propagating in the z direction, with the known electric field $E_{\mathrm{in}}(r_i) = E_i{}^0 g(r_i)$, is used for focusing with a convex lens. Here, $E_i{}^0$, r_i, and $g(r_i)$ are the peak electric field, the radial distance on the lens plane perpendicular to the z axis, and the normalized function, so $g(0) = 1$ for the electric field profile of the input beam.

Under the Fresnel condition it is possible to evaluate the electric field $E(x, y, z)$ near the focal region from the given input beam,[7] where the plane perpendicular to the z axis is denoted by x, y in a Cartesian coordinate system, i.e.,

$$E(r = \sqrt{x^2 + y^2}, z) = \frac{E_i{}^0}{\lambda f} \int g(r_i) J_0\left(2\pi \frac{r r_i}{\lambda f}\right) \exp\left[-i\pi \frac{z}{\lambda}\left(\frac{r_i}{f}\right)^2\right] 2\pi r_i \mathrm{d}r_i. \tag{1}$$

where λ, f, and J_0 are the wavelength of the laser, the focal length of the lens, and the zeroth order of Bessel function, respectively. This electric field can be also expressed as

$$E(r, z) = E_0[f_r(r, z) + i f_i(r, z)], \tag{2}$$

where E_0 denotes the electric field strength at the focal point, f_r and f_i are the real and the imaginary parts, respectively of the electric field profile, and $f_r(0, 0)$ is set to 1 for normalization.

The general expression for the electric field, E_e, at the exit of a sample of thickness L, linear refractive index n_0, linear absorption α, and third-order nonlinear susceptibility $\chi^{(3)} = \chi_R^{(3)} + i\chi_I^{(3)}$ was derived, which is Eq. (26) of Ref. 2. By considering only the low-irradiance limit so that both the nonlinear phase shift $\Delta\Phi = k\gamma I_0 L_e$ and the nonlinear absorption $\Delta\Psi = (\beta/2) I_0 L_e \ll 1$, one can approximate Eq. (26) of Ref. 2 as

$$E_e(r, z) = E(r, z)\exp(-\alpha L/2)(1 + iF\Delta\Phi - F\Delta\Psi), \tag{3}$$

where I_0 is the irradiance of the laser beam at the focal point, $F = f_r{}^2 + f_i{}^2$, $L_e = [1 - \exp(-\alpha L)]/\alpha$, $\gamma = \chi_R^{(3)}/2n_0{}^2\epsilon_0 c$, and $\beta = k\chi_I^{(3)}/n_0{}^2\epsilon_0 c$. Here k, ϵ_0 and c are the wave number of the light, a dielectric constant of vacuum, and the speed of light, respectively. From Eqs. (2) and (3) one can rewrite the complex field at the exit of the sample as

0740-3224/96/1202720-04$10.00

$$E_e(r, z) = E_0 \exp(-\alpha L/2)[(f_r - f_r F\Delta\Psi - f_i F\Delta\Phi) + i(f_i - f_i F\Delta\Psi + f_r F\Delta\Phi)]. \quad (4)$$

Because the transmitted electric field is detected at a long distance d from the sample, one can obtain the electric field E_d at the detector simply from the Fourier transformation of $E_e(r, z)$. Therefore the on-axis electric field $E_d(z = d \gg f)$ at the detector can be written as the surface integral of E_e, i.e.,

$$E_d(z = d) = \frac{1}{\lambda d} \int E_e \mathrm{d}s. \quad (5)$$

where $\mathrm{d}s = \mathrm{d}x\mathrm{d}y$. By using Eqs. (4) and (5) one can derive the normalized on-axis transmittance $T(z)$:

$$T(z) = 1 + \frac{2\left(\int f_i \mathrm{d}s \int f_r F \mathrm{d}s - \int f_r \mathrm{d}s \int f_i F \mathrm{d}s\right)}{\left(\int f_r \mathrm{d}s\right)^2 + \left(\int f_i \mathrm{d}s\right)^2} \Delta\Phi - \frac{2\left(\int f_r \mathrm{d}s \int f_r F \mathrm{d}s + \int f_i \mathrm{d}s \int f_i F \mathrm{d}s\right)}{\left(\int f_r \mathrm{d}s\right)^2 + \left(\int f_i \mathrm{d}s\right)^2} \Delta\Psi. \quad (6)$$

This result permits a straightforward evaluation of $T(z)$ for an arbitrary spatial input beam with circular symmetry. In particular, one can prove that $\int f_i \mathrm{d}s = 0$ for an input beam whose electric field profile has an expansion of only even powers of r_i, i.e., $g(r_i) = 1 + \sum_{n=1}^{\infty} c_n r_i^{2n}$ such as a top-hat, Airy, or Gaussian beam, where c_n and n denote the corresponding coefficient and positive integer, respectively. The detailed proof is shown in Appendix A. In this case $\int f_r \mathrm{d}s$ becomes a constant because $(\int f_r \mathrm{d}s)^2 + (\int f_i \mathrm{d}s)^2$ is a constant, independently of z. Furthermore, Eq. (6) is simplified to

$$T(z) = 1 - \frac{2\int f_i F \mathrm{d}s}{\int f_r \mathrm{d}s} \Delta\Phi - \frac{2\int f_r F \mathrm{d}s}{\int f_r \mathrm{d}s} \Delta\Psi, \quad (7)$$

permitting calculation of $T(z)$ with ease. If we define a sensitivity factor $\mathscr{S}_{\mathscr{Z}} \equiv \Delta T_{\mathrm{pv}}/\Delta\Phi$ as the ratio of the difference between the normalized peak-and-valley Z-scan transmittance ΔT_{pv} and $\Delta\Phi$ at the low irradiance for a nonzero $\chi_R^{(3)}$, it can be understood that $\mathscr{S}_{\mathscr{Z}}$ is only a function of the electric field profile of the input beam. It is found that $\mathscr{S}_{\mathscr{Z}} = 0.406$ and $\mathscr{S}_{\mathscr{Z}} = 1.02$ for Gaussian and top-hat beams, respectively, as reported previously.[2,6]

We carried out all Z-scan experiments by using a Q-switched Nd:YAG laser (Lumonics HY-750) of 8-ns pulse duration (FWHM) operating at a 10-Hz repetition rate. The spatial irradiance profile and the beam divergence of the output beam from the HY 750 laser were of an approximately top-hat shape, 8 mm in diameter and, 0.8 mrad. We obtained the nearly top-hat beam by passing the output of the laser beam through a circular aperture of 2.14-mm diameter. The measured irradiance profile is shown as open circles in Fig. 1. This beam was focused with a convex lens of focal length 10.5 cm. We measured the on-axis Z-scan transmittance by scanning a 1-mm quartz cuvette filled with CS_2. To satisfy the criteria for the on-axis detection we inserted the circular 1-mm-diameter aperture in front of a photodiode located 0.7 m from the lens, which corresponds to a linear transmittance of 1.2% when there is no sample. One of the experimental results for the normalized Z-scan transmittance for CS_2 with an on-axis irradiance at the focal point $I_0 = 1.3$ GW/cm^2 is shown as open circles in Fig. 2. We found that it is not trivial to get a symmetric pattern of the peak and valley experimentally because the pattern depends sensitively on the position of the pinhole for the on-axis detection. Note should be taken that the symmetry of the peak and valley is important for estimation of the complex nature of $\chi^{(3)}$. The cause of this disadvan-

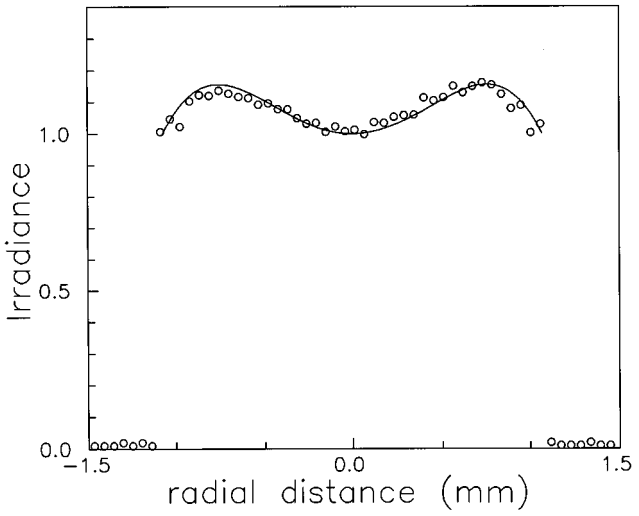

Fig. 1. Measured irradiance profile of a nearly top-hat-shaped beam (open circles). The solid curve is a best-fit function to the experimental data.

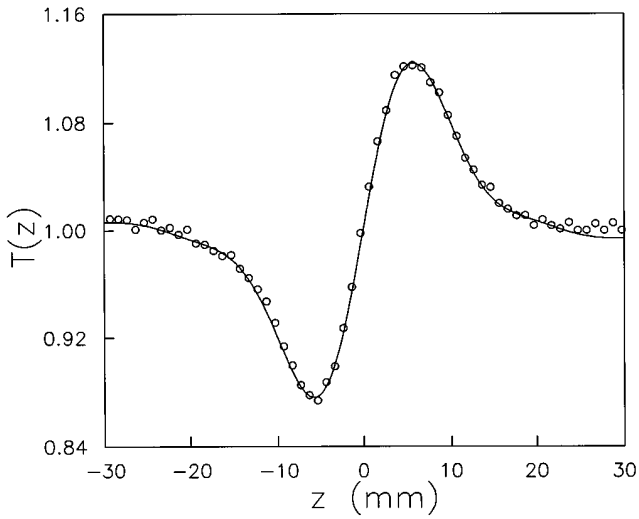

Fig. 2. Normalized on-axis Z-scan transmittance for the nearly top-hat beam with $I_0 = 1.3$ GW/cm^2. The solid curve is a numerical fit with $\Delta\Phi = 0.25$.

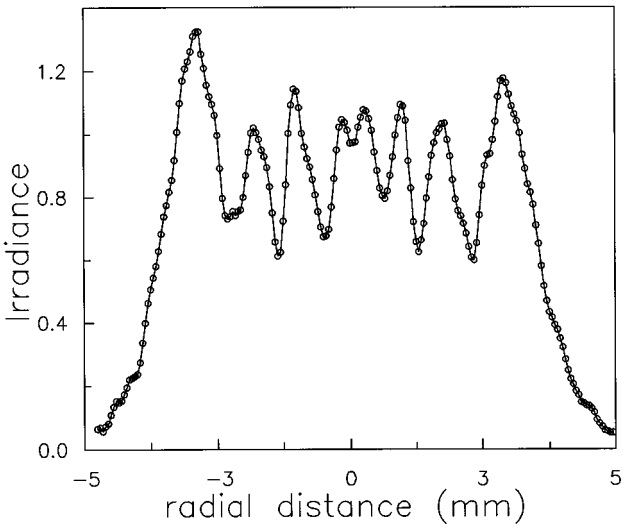

Fig. 3. Irradiance profile of the focused nearly top-hat beam measured 0.7 m from the lens.

tage can easily be understood from the overall irradiance profile of the focused, nearly top-hat beam in the far field (0.7 m away from the lens), which is shown in Fig. 3. As can be seen, there are several sharp peaks, so it is not easy to find the center experimentally for on-axis detection. This makes it difficult to measure an unknown complex $\chi^{(3)}$ of a given material. The complicated image in the far field arises from the fact that this irradiance pattern is the Fourier integral of the Airy function within a finite area because of experimental restriction such as limitations of the sample holder rather than the complete Airy function.

To obtain an Airy profile for the input beam we passed the output beam of the same laser through the 1-mm-diameter circular aperture (the input pinhole), followed by free-space propagation of 1.5 m. Then we used the central, intense part of this Airy beam (trimmed Airy beam) for the Z-scan experiment by locating another circular aperture of the correct radius (2.2 mm in our experiment) that corresponded to the first zero of the irradiance profile at a distance of 1.5 m from the input pinhole. The measured irradiance profile of this trimmed Airy beam is shown as open squares in Fig. 4. The solid curve is the theoretically fitted function of $[2J_1(x)/x]^2$. Note that the square of the Airy function shows almost perfect agreement with the corresponding experimental data. In Fig. 5, a typical on-axis Z-scan measurement made with a trimmed Airy beam is shown as open squares. Here the on-axis irradiance of the laser at the focal point is estimated to be $I_0 = 1.2$ GW/cm^2. It is easy to locate the detecting pinhole at the center of the far-field pattern of the trimmed Airy beam because the irradiance profile of the beam is observed to be the square of a trimmed Airy function within experimental error, as it should be, resulting in the definite symmetric nature of the peak and the valley experimentally. This should be an experimental advantage when one is using a trimmed Airy beam rather than a top-hat beam in Z-scan measurements of complex $\chi^{(3)}$.

For numerical analysis of Z-scan transmittance, to take into account that the irradiance profile of our input beam is slightly different from that of a top-hat, we use the following function $g(r_i)$ for the nearly top-hat beam:

$$g(r_i) = \begin{cases} 1 + 0.3[(r_i/a)^2 - (r_i/a)^4] & |r_i| \leq a \\ 0 & |r_i| > a \end{cases}, \quad (8)$$

where $a = 1.07$ mm. The square of Eq. (8), shown as the solid curve in Fig. 1, yields a close approximation of the corresponding experimental irradiance profile. By using Eqs. (1), (7), and (8) and the known value of $\chi^{(3)}$ of CS_2 (3.3×10^{-12} esu^2), we can obtain a consistent numerical result (with $\Delta\Phi = 0.25$), shown as the solid curve in Fig. 2,

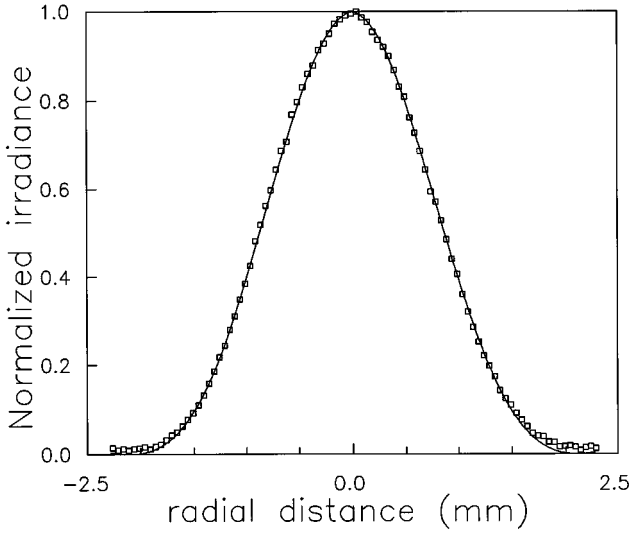

Fig. 4. Measured diffraction pattern for a circular aperture of 0.5-mm radius (open squares). The measurements were made 1.5 m from the aperture (input pinhole). The solid curve is the best fit to a square of the trimmed Airy function.

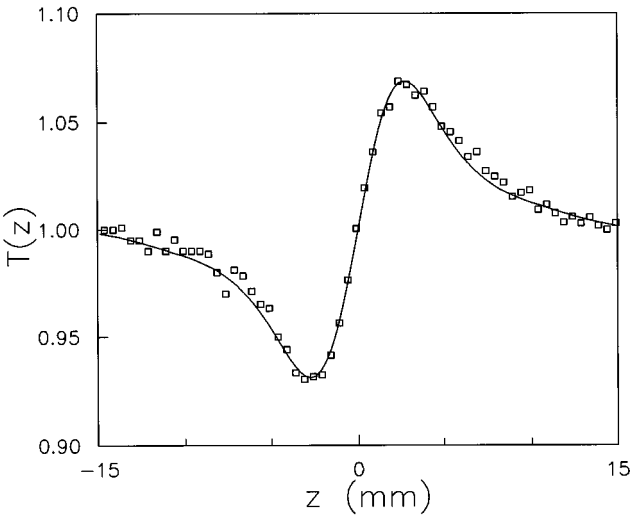

Fig. 5. Normalized on-axis Z-scan transmittance for the trimmed Airy beam with $I_0 = 1.2$ GW/cm^2. The solid curve is the numerical fit with $\Delta\Phi = 0.23$.

with the experimental data for the Z-scan transmittance. We also found that $\mathscr{S}_{\mathscr{Z}} = 0.94$ for our nearly top-hat beam, which is slightly less than that for the perfect top-hat shape. Finally, we evaluated the numerical Z-scan transmittance for a trimmed Airy beam by the same method. The result (with $\Delta\Phi = 0.23$) is drawn as the solid curve in Fig. 5, which again shows good agreement with the experimental data. $\mathscr{S}_{\mathscr{Z}}$ is found to be 0.61, which is 1.5 times larger than that for a Gaussian beam. Furthermore, the convergence in the numerical evaluation of the Z-scan transmittance is remarkably faster than that for a top-hat beam, leading to accurate and fast numerical results.

In summary, we have developed a systematic method for the numerical evaluation of on-axis Z-scan transmittance with an arbitrary circularly symmetric input beam. We found that a trimmed Airy beam is practically advantageous over a top-hat beam for Z-scan experiments, not only because it has the symmetric nature of an irradiance profile but also because it has a fast convergence nature for the numerical evaluation of Z-scan transmittance.

APPENDIX A: PROOF OF $\int f_i \mathrm{d}s = 0$

Here we show that $\int_0^\infty f_i \mathrm{d}s = 0$ for $g(\rho) = 1 + \Sigma_{n=1}^{\infty} c_n \rho^{2n}$ and the finite a, where a is the radial distance for the input beam beyond which the irradiance of the input beam does not exist. From Eq. (1), the electric field profile near the focal region can be rewritten as

$$E(r, z) = \frac{E_i^0}{\lambda f} 2\pi a^2 \int_0^1 g(\rho) J_0(v\rho) \exp(-iq\rho^2) \rho \mathrm{d}\rho, \tag{A1}$$

where $\rho = r_i/a$, $v = (2\pi a/\lambda f)r$ and $q = \pi(z/\lambda)(a/f)^2$.

Therefore one can prove that $\int_0^\infty f_i \mathrm{d}s = 0$ by showing that the integral $I_{\mathrm{Im}\, f}$ vanishes, i.e.,

$$I_{\mathrm{Im}\, f} = \lim_{b\to\infty} \int_0^b \left[\int_0^1 g(\rho) \sin(q\rho^2) J_0(v\rho) \rho \mathrm{d}\rho \right] v \mathrm{d}v. \tag{A2}$$

This integral can be carried out with respect to v first. Then one can find that

$$I_{\mathrm{Im}\, f} = \lim_{b\to\infty} b \int_0^1 g(\rho) \sin(q\rho^2) J_1(b\rho) \mathrm{d}\rho. \tag{A3}$$

Using the facts that $g(\rho) = 1 + \Sigma_{n=1}^{\infty} c_n \rho^{2n}$ and $\sin(q\rho^2) = \Sigma_{n=1}^{\infty} (-1)^{n-1} [(q\rho^2)^{2n-1}/(2n-1)!]$, one can find that $g(\rho)\sin(q\rho^2)$ can be expanded in the even powers of ρ, i.e.,

$$g(\rho)\sin(q\rho^2) = \sum_{n=1}^{\infty} d_n \rho^{2n}, \tag{A4}$$

where d_n is the relevant coefficient.

By substituting Eq. (A4) into Eq. (A3), one can also find that the integral $I_{\mathrm{Im}\, f}$ is a linear combination of the following integrals:

$$I_n = \lim_{b\to\infty} b \int_0^1 \rho^{2n} J_1(b\rho) \mathrm{d}\rho. \tag{A5}$$

Integrating by parts, one can show that Eq. (A5) has the analytical expression

$$I_n = \lim_{b\to\infty} \sum_{s=1}^{n} \left(-\frac{2}{b} \right)^{s-1} \frac{(n-1)!}{(n-s)!} J_{s+1}(b), \tag{A6}$$

which is zero for any positive integer n.

ACKNOWLEDGMENTS

B. K. Rhee thanks all the associates of the Center for Research in Electro-Optics and Lasers, University of Central Florida, for their kind hospitality during his sabbatical there. The present studies were supported in part by the Basic Science Research Institute Program, Ministry of Education of Korea project BSRI-'95-2415.

REFERENCES

1. M. Sheik-Bahae, A. A. Said, and E. W. Van Stryland, "High-sensitivity, single-beam n_2 measurements," Opt. Lett. **14**, 955 (1989).
2. M. Sheik-Bahae, A. A. Said, T. H. Wei, D. J. Hagan, and E. W. Van Stryland, "Sensitive measurement of optical nonlinearities using a single beam," IEEE J. Quantum Electron. **26**, 760 (1990).
3. A. A. Said, M. Sheik-Bahae, D. J. Hagan, T. H. Wei, J. Wang, J. Young, and E. W. Van Stryland, "Determination of bound-electronic and free-carrier nonlinearities in ZnSe, GaAs, CdTe, and ZnTe," J. Opt. Soc. Am. B **9**, 405 (1991).
4. L. Yang, R. Dorsinville, Q. Z. Wang, P. X. Ye, and R. R. Alfano, "Excited-state nonlinearity in polythiophene thin films investigated by the Z-scan technique," Opt. Lett. **17**, 323 (1992).
5. B. A. Rockwell, W. P. Roach, M. E. Rogers, M. W. Mayo, and C. A. Toth, "Nonlinear refraction in vitreous humor," Opt. Lett. **18**, 1792 (1993).
6. W. Zhao and P. Palffy-Muhoray, "Z-scan technique using top-hat beams," Appl. Phys. Lett. **63**, 1613 (1993).
7. M. Born and E. Wolf, *Principles of Optics*, 6th ed. (Pergamon, Oxford, 1980), Sec. 8.8.